THE JOURNAL OF BIOLOGICAL CHEMISTRY VOL. 286, NO. 31, pp. 27582–27593, August 5, 2011

Molecular Mechanism of the E99K Mutation in Cardiac Actin (*ACTC* Gene) That Causes Apical Hypertrophy in Man and Mouse*[S]

Received for publication, April 18, 2011, and in revised form, May 18, 2011 Published, JBC Papers in Press, May 26, 2011, DOI 10.1074/jbc.M111.252320

Weihua Song[‡], Emma Dyer[‡], Daniel J. Stuckey[‡], O'Neal Copeland[‡], Man-Ching Leung[‡], Christopher Bayliss[‡], Andrew Messer[‡], Ross Wilkinson[‡], Jordi Lopez Tremoleda[§], Michael D. Schneider[‡], Sian E. Harding[‡], Charles S. Redwood[¶], Kieran Clarke[‖], Kristen Nowak[**], Lorenzo Monserrat[‡‡], Dominic Wells[§§], and Steven B. Marston[‡1]

From the [‡]National Heart and Lung Institute, Imperial College London, London SW32 6LY, United Kingdom, the [¶]Department of Cardiovascular Medicine, University of Oxford, Oxford OX3 9DU, United Kingdom, the [**]Center for Medical Research, University of Western Australia, Nedlands, Western Australia 6009, Australia, the [‡‡]Cardiology Department, Complejo Hospitalario Universitario Juan Canalejo, A Coruña 15006, Spain, the [§]Medical Research Council Clinical Sciences Centre, Imperial College London, London W12 0NN, United Kingdom, the [§§]Centre for Neuroscience, Imperial College London, London W12 0NN, United Kingdom, and the [‖]Department of Physiology, Anatomy, and Genetics, University of Oxford, Oxford OX1 3PT, United Kingdom

We generated a transgenic mouse model expressing the apical hypertrophic cardiomyopathy-causing mutation *ACTC* E99K at 50% of total heart actin and compared it with actin from patients carrying the same mutation. The actin mutation caused a higher Ca^{2+} sensitivity in reconstituted thin filaments measured by *in vitro* motility assay (2.3-fold for mice and 1.3-fold for humans) and in skinned papillary muscle. The mutation also abolished the change in Ca^{2+} sensitivity normally linked to troponin I phosphorylation. MyBP-C and troponin I phosphorylation levels were the same as controls in transgenic mice and human carrier heart samples. *ACTC* E99K mice exhibited a high death rate between 28 and 45 days (48% females and 22% males). At 21 weeks, the hearts of the male survivors had enlarged atria, increased interstitial fibrosis, and sarcomere disarray. MRI showed hypertrophy, predominantly at the apex of the heart. End-diastolic volume and end-diastolic pressure were increased, and relaxation rates were reduced compared with nontransgenic littermates. End-systolic pressures and volumes were unaltered. ECG abnormalities were present, and the contractile response to β-adrenergic stimulation was much reduced. Older mice (29-week-old females and 38-week-old males) developed dilated cardiomyopathy with increased end-systolic volume and continuing increased end-diastolic pressure and slower contraction and relaxation rates. ECG showed atrial flutter and frequent atrial ectopic beats at rest in some *ACTC* E99K mice. We propose that the *ACTC* E99K mutation causes higher myofibrillar Ca^{2+} sensitivity that is responsible for the sudden cardiac death, apical hypertrophy, and subsequent development of heart failure in humans and mice.

Hypertrophic cardiomyopathy (HCM)[2] is the most commonly inherited cardiomyopathy with an estimated incidence of 1 in 500 of the population (1, 2). More than 600 mutations have been discovered to be associated with HCM with all but a few in the genes coding for the contractile apparatus of the myofibril, predominantly myosin-binding protein C and β-myosin heavy chain (3–6). Eleven mutations have been identified in the cardiac actin gene, *ACTC* (7–11), including the E99K mutation that has been intensively investigated as it has been shown to co-segregate with an unusual apical hypertrophic phenotype (12, 13). HCM is defined clinically as the presence of unexplained ventricular hypertrophy; usually the thickening is most prominent in the interventricular septum, but other pathologies can also occur, such as apical and concentric hypertrophy or left ventricular noncompaction. Electrocardiogram abnormalities are also common, including abnormal repolarization or Q-waves (for normal HCM). Histologically, HCM is characterized by myocyte disarray and interstitial fibrosis. The hypertrophy leads to decreased left ventricular volume and may cause outflow tract obstruction, which along with impaired relaxation can lead to heart failure.

HCM is also associated with sudden cardiac death due to arrhythmias especially in young active adults. The overall risk of fatal complications of HCM is 1–2% per year (2, 14). Although hypertrophy and sudden cardiac death are both caused by HCM mutations, the connection between them is unclear. The mutant protein in HCM is expressed from birth but is compensated for in almost all cases until adolescence, and sometimes symptoms never develop. This variable penetrance indicates that genetic background is significant to the outcome of HCM mutations.

We and others have expended much effort to determine how HCM mutations alter myofibrillar function to induce the phe-

* This work was funded by grants from the British Heart Foundation, a generous donation from The Dr. E. G. J. Olsen Charitable Fund, the British Heart Foundation Centre of Research Excellence, and the 7th Framework Program of the European Union Grant 241577 ("BIG-HEART").

[S] The on-line version of this article (available at http://www.jbc.org) contains supplemental Methods, data A–J, and additional references.

[1] To whom correspondence should be addressed: National Heart and Lung Institute, Dovehouse St., London SW3 6LY, United Kingdom. Tel.: 442073518147; Fax: 442078233392; E-mail: s.marston@imperial.ac.uk.

[2] The abbreviations used are: HCM, hypertrophic cardiomyopathy; IVMA, *in vitro* motility assay; TnI, troponin I; TnT, troponin T; APD, action potential duration; EDV, end-diastolic volume; NTG, nontransgenic; TG, transgenic; TRITC, tetramethylrhodamine isothiocyanate; EDV, end-diastolic volume; SV, stroke volume; EF, ejection fraction; CO, cardiac output; DCM, dilated cardiomyopathy.

notype. It has been widely supposed that mutant protein would be expressed in the heart at up to 50% of total protein and that it exerts its pathological effects by acting as a poison peptide that alters normal function. Direct measurements in human heart tissue have confirmed the poison peptide hypothesis in a few cases (15–17). The challenge is to explain how over 600 different mutations can cause the same phenotype. *In vitro* studies, either using recombinant proteins or proteins from transgenic mouse models, have shown that HCM mutations can cause a higher Ca^{2+} sensitivity of the contractile apparatus, a faster cross-bridge turnover rate, and incomplete relaxation at 10^{-9} M Ca^{2+} (18–21). Thus HCM mutations seem to involve a "gain of function" that would lead to a hypercontractile cardiac phenotype, as is indeed seen in many younger HCM patients.

A problem with most of these *in vitro* studies is that when the mutant protein is obtained from bacterial or baculovirus expression systems it will not have native post-translational modifications, especially phosphorylation. Moreover, measurements are usually made in heterologous systems with the mutation introduced into mouse or human isoforms of a protein and then tested in a system containing partner proteins from a different species. Recent studies have shown that species, isoform, and post-translational modification context can have a significant influence on the functional effect of a mutation (16, 22, 23).

This study reports our observations on a transgenic mouse model of HCM due to the E99K mutation in cardiac actin that avoids most of the problems with interpretation of data as described above (the mutation is in codon 101 of the *ACTC* gene, but two N-terminal amino acids are removed by post-translational processing to form the mature protein (24)). Uniquely among the contractile proteins, both skeletal and cardiac actin have identical amino acid sequences in humans and mice and an identical isoform distribution in heart (25% *ACTA1* and 75% *ACTC*) (25, 26). *In vivo* there are no post-translational modifications of actin that regulate activity. We have expressed the *ACTC* mutant without any adducts that could alter function at a level similar to the level expressed in patients with this mutation. A further advantage of the *ACTC* mutation is that transgenic expression of actin in the heart has been extensively studied, and it has been demonstrated that overexpression of actin in the heart does not lead to any alteration in the stoichiometry or structure of the myofibrils or any accumulation of actin in the cytoplasm (27). In functional studies, we have reconstituted thin filaments with mutant actin and tropomyosin and troponin from human heart muscle so that we can reproduce exactly the human mutant thin filament.

The *ACTC* E99K mutation is the subject of an extensive ongoing clinical study with 76 mutation carriers in 10 families currently identified (13). This mutation is associated with a unique form of hypertrophy where the apex of the heart is thickened, with a phenotype overlapping both HCM and left ventricular hypertrabeculation/noncompaction. We have therefore been able to compare the phenotype of our transgenic mice with the patient population. In addition, we have obtained patient biopsies, enabling us to perform the first direct comparison of the functional properties of an HCM-causing mutation in hearts from humans and mice at the molecular level.

Here, we show that the *ACTC* E99K mutant mice have a distinctive phenotype with increased myofilament Ca^{2+} sensitivity and a blunting of the response to PKA phosphorylation of troponin I at the single filament level. The mice develop apical hypertrophy progressing to dilated cardiomyopathy, and a high proportion die suddenly at 4–6 weeks old. Many of these characteristics reproduce the phenotype of patients with this mutation.

MATERIALS AND METHODS

The generation of transgenic mice, using the α-MyHC promoter, and their phenotypic characterization by echocardiography, electrocardiography, magnetic resonance imaging, and conductance catheter is described in the supplemental material. Force was measured in mouse papillary muscle strips as described by Song *et al.* (28) (see supplemental material). All procedures were performed in accordance with the United Kingdom Animals (Scientific Procedures) Act of 1986.

Polymeric actin was isolated from nontransgenic and *ACTC* E99K mice and from donor human hearts and E99K patient biopsies as described by Song *et al.* (28). Thin filaments were reconstituted with actin, native human troponin, and tropomyosin. Human cardiac troponin was prepared from donor heart myofibrils using an anti-TnI antibody affinity column as described by Messer *et al.* (29). Phosphorylation of troponin I and troponin T was measured by staining SDS-polyacrylamide gels of troponin or myofibrils with the Pro-Q Diamond phosphoprotein-specific stain followed by Coomassie Blue total protein stain as described previously (29) or by phosphate affinity SDS-PAGE as described by Messer *et al.* (30). Troponin was dephosphorylated by treatment with acid phosphatase (Sigma) as described previously (29). Human cardiac tropomyosin was isolated as described by Knott *et al.* (31).

The *in vitro* motility assay technique was used to study TRITC-phalloidin-labeled actin (actin-ϕ) filaments moving over immobilized rabbit fast muscle heavy meromyosin (100 μg/ml) on a dichlorodimethylsilane-coated surface (32, 33). Thin filament movement was observed at 28 °C in 50 mM KCl, 25 mM imidazole HCl, pH 7.4, 4 mM $MgCl_2$, 1 mM EDTA, 5 mM DTT, 0.5 mg/ml BSA, 0.1 mg/ml glucose oxidase, 0.02 mg/ml catalase, 3 mg/ml glucose, 0.5% methylcellulose, 5 mM Ca/EGTA buffer (range 1 nM to 3.7 μM Ca^{2+}), 1 mM MgATP, and troponin at the appropriate concentrations. Filament movement was recorded and analyzed as described previously (34). For complete details see the supplemental material.

Heart muscle biopsies were obtained from the hearts of two heterozygous carriers of the *ACTC* E99K mutation undergoing surgery related to the disease-causing mutation. Sample 1 was from a heart transplant for end-stage heart failure, and sample 2 was from a patient undergoing surgery for atrial septal defect (supplemental data A). Donor heart tissue was obtained from hearts where no suitable transplant recipient was found. These patients had no history of cardiac disease and normal electrocardiography (ECG) and ventricular function. Ethical approval was obtained from Comité Ético de Investigatión Clínica de Galicia and St. Vincent's Hospital, Sydney, Australia. This investigation conforms to the principles of the Declaration of Helsinki.

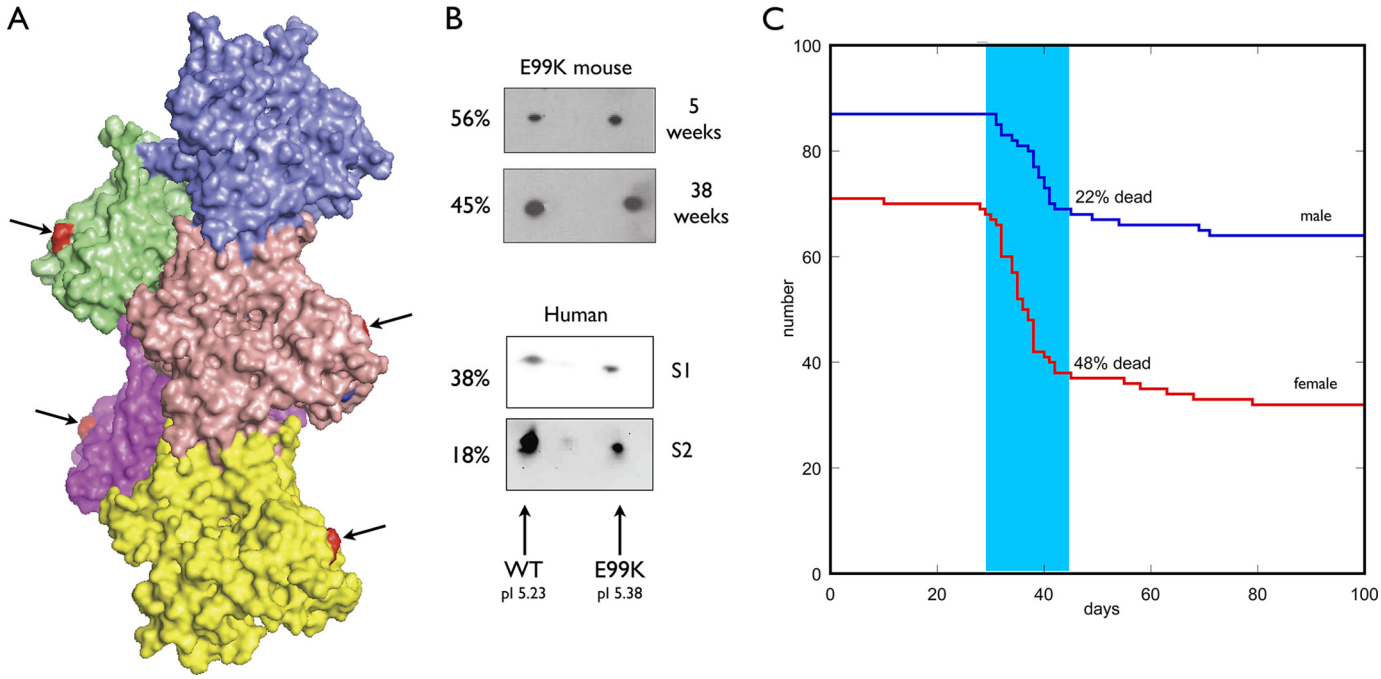

FIGURE 1. *A,* location of the E99K mutation in the actin filament. Model of a 5-actin monomer segment of the actin filament (Actin_Model.pdb (60)). Surface rendering using PyMol. Glutamic acid 99 (*arrows*) is shown in *red* at the surface on the edge of subdomain 1. *B,* two-dimensional electrophoresis demonstrating the expression of mutant actin in myofibrils from transgenic mouse heart and patient heart samples 1 (*S1*) and 2 (*S2*). *C,* Kaplan-Meir plot showing mortality in male and female *ACTC* E99K mice.

RESULTS

Generation and Characterization of the E99K Mice—Two mouse lines tested positive for the *ACTC* E99K mutation. The level of expression, assessed by two-dimensional electrophoresis, was 11–50%. One line that consistently expressed 50 ± 5% E99K actin was investigated further (Fig. 1). The mice appeared healthy when born; litter size (8 ± 2) and male to female ratio (53:47) were normal. Transgenic/nontransgenic mouse ratios were 106:182 at birth. The E99K transgenic mice exhibited a high death rate over a short period between 28 and 45 days; 48% of all the females died in this period and 22% of the males (Fig. 1). After this period, the survivors showed a low level of sporadic mortality that is more prominent in females than males and is higher than the nontransgenic (NTG) littermates.

The 21-week-old male *ACTC* E99K hearts had enlarged left and right atria, especially the left atrium (Fig. 2). Myocyte disarray and interstitial fibrosis was apparent in ventricular muscle (Fig. 2). At 29 and 38 weeks, *ACTC* E99K mice started showing body weight loss, and the hearts were enlarged compared with their littermates with a significantly increased heart/body weight ratio (supplemental data G). Three of 5 female *ACTC* E99K mice and 2 of 5 male *ACTC* E99K mice had severe hydrothorax with enlarged and dark-colored left atria with scar tissue. Under magnetic resonance imaging (MRI), some of the mice showed that the hearts were in the middle or the right side of their chests (supplemental data B).

Molecular Phenotype of E99K Actin from Transgenic Mice—Protein and phosphoproteins in myofibrils from nontransgenic and *ACTC* E99K mouse hearts were analyzed by SDS-PAGE at 5, 21, 29, and 38 weeks. The protein content of the myofibrils was identical with no evidence for the loss of actin or actin-binding proteins in the *ACTC* E99K mouse myofibrils (Fig. 3*A*). Staining the gels with Pro-Q Diamond showed that myosin-binding protein C (MyBP-C), troponin T (TnT), troponin I (TnI), and myosin light chain 2 (MLC-2) were the predominant phosphoproteins and that the phosphorylation levels in *ACTC* E99K hearts were not significantly different from NTG between 5 and 29 weeks (Fig. 3*B*).

The phosphorylation of troponin I in myofibrils was investigated in more detail using the phosphate affinity SDS-PAGE technique (Fig. 3*C*). In 21-week-old mice, troponin I phosphorylation was identical in NTG and *ACTC* E99K; troponin I was predominantly mono (1P)- and bisphosphorylated (2P) (NTG, 36 ± 2% 2P, 47 ± 2% 1P; *ACTC* E99K, 37 ± 1% 2P; 42 ± 2% 1P), and calculated total phosphorylation was 1.18 ± 0.03 mol of phosphate/mol of TnI in NTG and 1.17 ± 0.02 in *ACTC* E99K myofibrils ($p = 0.772$, unpaired t test). At 38 weeks, where mice showed symptoms of heart failure, troponin I phosphorylation was significantly reduced compared with NTG (total TnI phosphorylation of *ACTC* E99K/NTG = 0.64, $p = 0.001$).

We made functional measurements on thin filaments incorporating actin from NTG or *ACTC* E99K mice using the quantitative *in vitro* motility assay. We isolated polymeric actin filaments directly from NTG and *ACTC* E99K mouse hearts by isolating thin filaments and then stripping off regulatory proteins; in our previous studies, monomeric mouse cardiac actin, isolated by the conventional acetone powder method, did not yield mutant-containing thin filaments (28).

E99K actin filament sliding speed on immobilized rabbit fast skeletal muscle heavy meromyosin was 8% slower than wild-type actin (WT = 2.84 ± 0.11 μm/s and *ACTC* E99K = 2.61 ± 0.10 μm/s, $n = 14$, $p = 0.004$ paired t test). In the presence of 40 mM tropomyosin, sliding speed increased by 10% for E99K actin (to 2.84 ± 0.18 μm/s) and 6.5% for wild-type actin (to 2.95 ±

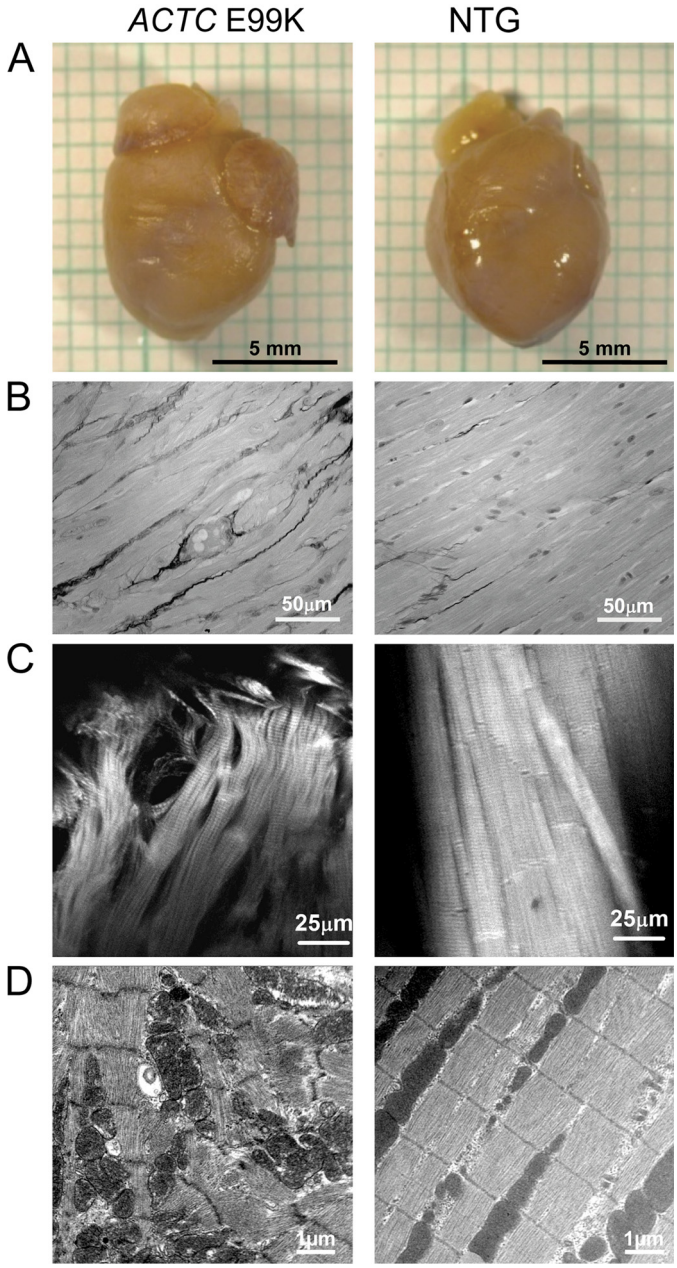

FIGURE 2. **Morphology of 21-week-old male mouse hearts.** *A,* isolated hearts: the *ACTC* E99K mouse heart shows enlarged atria but normal ventricles. *B,* fibrosis in mouse heart visualized in Sirius red-stained sections. The E99K mice show more interstitial fibrosis and less well ordered myocytes. *C,* confocal microscopy of mouse papillary muscle. Both samples were stretched to a sarcomere length of 2.1 μm; actin was labeled with TRITC-phalloidin. *D,* electron microscopy of apical region of a mouse heart. The *ACTC* E99K mouse showed significant myocyte disarray.

0.14 μm/s, so that the difference between the two actins became insignificant ($n = 10$, $p = 0.34$, paired t test; see supplemental data H).

Thin filaments were reconstituted with mouse actin, human cardiac tropomyosin, and human donor heart troponin. The fraction of motile filaments, measured with both NTG and E99K actin, was fully Ca^{2+}-regulated, but sliding speed changed by less than 40% between relaxing and activating Ca^{2+} concentrations. This pattern of results is typical of thin filaments in our IVMA system that uses a trimethysilane-coated surface (28, 32, 35). The motility of NTG and E99K actin-containing thin filaments was indistinguishable at both activating and relaxing Ca^{2+} concentrations (supplemental data H). When the Ca^{2+} concentration dependence of thin filament motility was assayed, the E99K actin thin filaments had a consistently higher Ca^{2+} sensitivity (EC_{50} wild-type/EC_{50} E99K actin = 2.3 ± 0.6, $p = 0.02$, see Fig. 4 and supplemental data I).

We also measured Ca^{2+} regulation of isometric force in skinned mouse heart papillary muscles. In this system, the Ca^{2+} sensitivity of *ACTC* E99K mouse heart muscle was again significantly higher than NTG heart muscle (EC_{50} NTG muscle/EC_{50} *ACTC* E99K muscle = 1.30 ± 0.03, $p = 0.003$, see Fig. 4). The difference was less than in the isolated thin filaments, as has been frequently observed with HCM-causing mutations (36). The maximum force in skinned papillary muscles tended to be lower in the *ACTC* E99K samples (NTG 27 ± 6 kilonewtons/m^2, *ACTC* E99K 20 ± 9 kilonewtons/m^2, $p = 0.124$).

We used IVMA to determine the effect of a change of troponin I phosphorylation on Ca^{2+} sensitivity by treating donor heart troponin (1.6 mol of phosphate/mol) with phosphatases to reduce TnI phosphorylation levels to less than 0.2 mol of phosphate/mol (Fig. 4*D* and supplemental data I). Thin filaments reconstituted with wild-type actin and dephosphorylated troponin showed a 2.9 ± 0.3-fold higher Ca^{2+} sensitivity compared with native phosphorylated troponin (actin from five hearts assayed, $p = 0.03$, paired t test), but this characteristic response to dephosphorylation of troponin I of Ser-23/24 (PKA sites) was not observed with E99K actin. The Ca^{2+} sensitivity of E99K actin-containing thin filaments with dephosphorylated troponin was not significantly higher than with natively phosphorylated troponin (EC_{50} phosphorylated E99K Tn/EC_{50} dephosphorylated E99K Tn = 1.14 ± 0.06, actin from four hearts assayed, $p = 0.16$, paired t test, see Fig. 4). Thus, the E99K actin mutation increases Ca^{2+} sensitivity of thin filaments and blunts the response to changes in troponin I phosphorylation.

Cardiac Contractility in 21-Week-old Male ACTC E99K Survivors—We investigated the effect of the E99K mutation in cardiac actin on the contraction of mouse hearts *in situ*. MRI, echocardiography, ECG, and conductance catheter studies were performed on male 21-week-old mice (Fig. 5, Table 1, and supplemental data C–E). Compared with NTG littermates, 21-week-old *ACTC* E99K mouse hearts had significant hypertrophy in the apical region of the left ventricular posterior wall and interventricular septum, with no differences at the base. Wall thickening during contraction was significantly reduced in the apical region in both the septum and left ventricular posterior wall of *ACTC* E99K heart compared with NTG but was unaltered at the base. End-diastolic volume (EDV), stroke volume (SV), ejection fraction (EF), and cardiac output (CO) were lower in *ACTC* E99K mice (EDV, 52.71 ± 3.40 *versus* 66.04 ± 3.89, $p < 0.01$; SV, 26.69 ± 2.65 *versus* 40.67 ± 2.83, $p < 0.01$; EF, 50.27 ± 2.27 *versus* 62.19 ± 3.54, $p < 0.01$; CO, 9.06 ± 0.76 *versus* 17.22 ± 1.06, $p < 0.001$). *ACTC* E99K mice had higher end-diastolic pressure (5.693 ± 1.412 *versus* 1.364 ± 0.610, $p < 0.05$) than NTG littermates, although end-systolic pressure (73.89 ± 4.35 *versus* 75.42 ± 3.43, $p > 0.05$) was the same. End-systolic elastance (6.284 ± 1.231 *versus* 12.08 ±

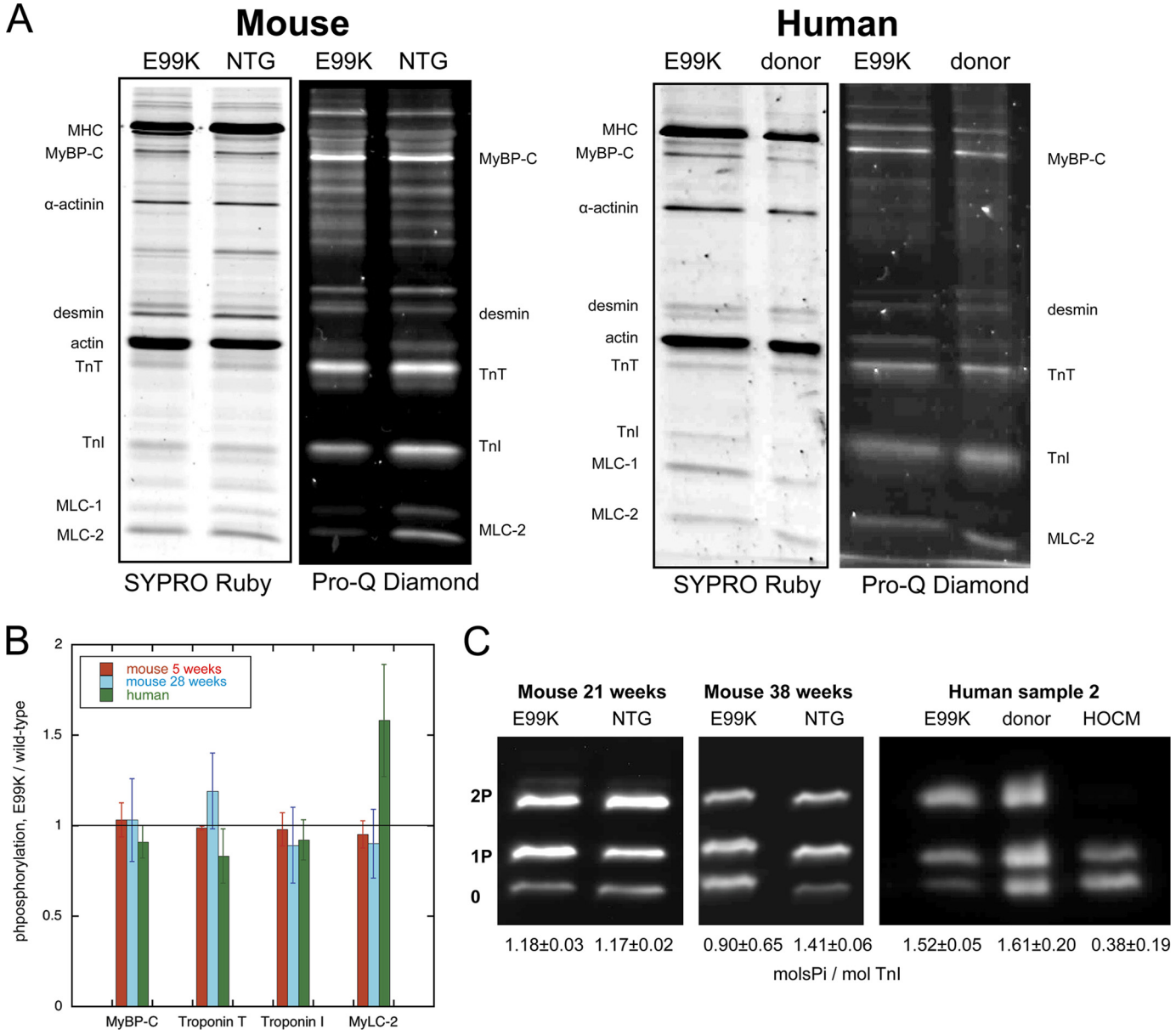

FIGURE 3. **SDS-PAGE analysis of myofibrillar proteins and phosphoproteins.** *A,* myofibril fraction of heart muscle separated by SDS-PAGE and stained successively with Pro-Q Diamond phosphoprotein stain and SYPRO Ruby total protein stain. *Left,* NTG and *ACTC* E99K mouse heart myofibrils (38 weeks male). *Right,* donor and *ACTC* E99K heart sample 2 myofibrils. *B,* relative phosphorylation levels for MyBP-C, troponin T, troponin I, and MLC-2 for human sample 2 and *ACTC* E99K mice at 5 and 29 weeks as determined from Pro-Q Diamond-stained SDS-PAGE as in *A*. Means ± S.E. of 4–6 measurements are shown. *C,* phosphate affinity SDS-PAGE analysis of troponin I phospho-species. *Left,* comparison of troponin I phosphorylation in 21-week-old female *ACTC* E99K and NTG mouse myofibrils. *Right,* comparison of troponin I phosphorylation in myofibrils from *ACTC* E99K sample 2, donor heart, and a typical interventricular septum sample from a patient with hypertrophic obstructive cardiomyopathy (*HOCM*).

1.307, $p < 0.05$) was reduced, and end-diastolic pressure volume relationship (0.714 ± 0.116 *versus* 0.217 ± 0.047, $p < 0.01$) and Tau_g (17.72 ± 1.21 *versus* 9.518 ± 1.023, $p < 0.001$) were increased. Taken together, these data suggest apical hypertrophy with left ventricular diastolic dysfunction in 21-week-old male *ACTC* E99K mouse heart.

Echocardiography of 21-week-old male *ACTC* E99K mice revealed a blunted response to β-adrenergic stimulation, with a less pronounced increase in heart rate, wall thickening, and fractional shortening compared with NTG mice (Fig. 5). No significant arrhythmia was recorded in 21-week-old male *ACTC* E99K mice ($n = 6$) using lead II ECG; however, T-wave flattening occurred in the majority of *ACTC* E99K mice, making measurements of QT intervals impossible (Fig. 6). Deep S-wave (1 mouse) and double S-waves (1 mouse) were recorded, indicating intraventricular conduction abnormalities in some *ACTC* E99K mice.

Changes in Cardiac Contractility with Age—ACTC E99K mice were further compared with NTG mice at 29 and 38 weeks old using MRI, echocardiography, and conductance catheter. Table 2 summarizes the changes in cardiac parameters in *ACTC* E99K mice expressed relative to the NTG littermates. Where a single parameter was measured by several techniques (for example EDV) the percentage change in the parameters were essentially the same, although the absolute magnitude could be different for technical reasons (for instance MRI

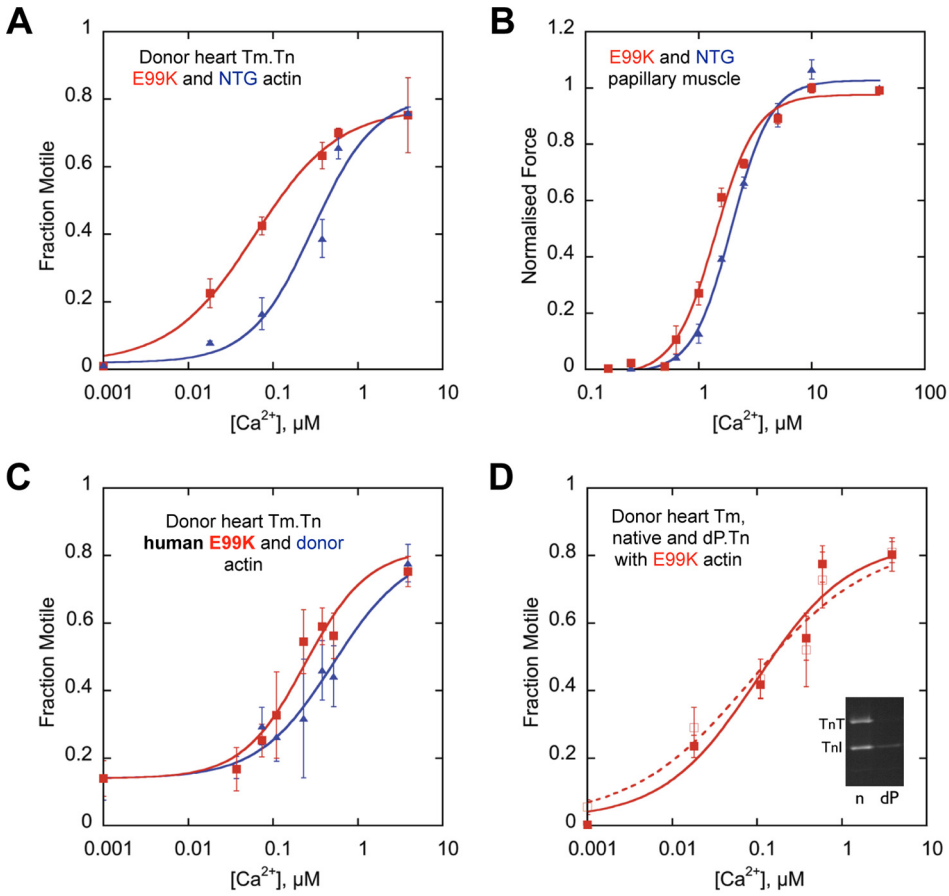

	number of hearts	number of assays		Wild-type actin	E99K actin	p , paired t test
skinned trabecula muscle	4	4	EC_{50}, isometric tension, μM	1.93±0.02	1.48±0.09	p=0.0027
Actin.Tm.Tn	5	5	EC_{50}, fraction motile, μM	0.35±0.09	0.15±0.05	p=0.02
Actin.Tm.Tn Human sample 2	1	5	EC_{50}, fraction motile, μM	0.42±0.10	0.34±0.12	p=0.017

FIGURE 4. **Ca^{2+} activation curves comparing *ACTC* E99K (*red squares*) with wild-type actin (*blue triangles*).** Standard error of 4–6 measurements is plotted. *Solid line* is best fit to the Hill equation; calculated parameters are shown in the *table* below. *A,* thin filaments reconstituted with *ACTC* E99K or NTG mouse actin, donor heart tropomyosin (*Tm*) and troponin (*Tn*), measured by *in vitro* motility assay. *B,* isometric force from *ACTC* E99K or NTG mouse heart papillary muscle strips. *C,* thin filaments reconstituted from actin from human *ACTC* E99K sample 2 or donor with donor heart tropomyosin and troponin, measured by *in vitro* motility assay. *D,* thin filaments reconstituted with *ACTC* E99K mouse actin, donor heart tropomyosin, and natively phosphorylated donor (*filled squares, solid line*) or dephosphorylated donor troponin (*open squares, dotted line*), measured by *in vitro* motility assay. *Inset,* Pro-Q Diamond-stained SDS-PAGE showing phosphorylated TnI and TnT in donor heart and absence of phosphorylation in the dephosphorylated donor troponin. The *table* shows the mean values of EC_{50}; data from individual experiments are given in supplemental data I and J.

always records a much higher volume than Millar catheter (37)).

We found a different time course of development of cardiac contractile dysfunction in male and female *ACTC* E99K mice (Table 2 and supplemental data B and E–G). 29-Week-old male *ACTC* E99K had a similar phenotype to 21-week-old mice with increased wall thickness and reduced EDV, SV, EF, and CO compared with controls. At 38 weeks, the male *ACTC* E99K mice also had increased end-systolic volume and Tau_g, and reduced dV/dt_{min} and dV/dt_{max} compared with NTG mice indicating both impaired myocardial contraction and relaxation. At this stage, the male mouse heart was progressing toward dilated cardiomyopathy.

At 29 weeks old, the female *ACTC* E99K mice retained the reduced EDV, SV, EF, and CO but additionally showed evidence of progression toward dilated cardiomyopathy, with increased end-systolic volume and Tau_g and reduced dV/dt_{min} relative to NTG. 38-Week-old female *ACTC* E99K mice had further increased EDV and end-systolic volume and lower EF, suggesting left ventricular remodeling and progression to dilated cardiomyopathy with diastolic dysfunction, impaired contraction, and relaxation.

At 29 weeks old, ECG recordings showed frequent episodes of atrial ectopic fibrillation in 7/8 male and 2/5 female *ACTC* E99K mice. Atrial flutter at steady status was present in 2/8 male and 1/5 female *ACTC E99K* mice. The T-wave was iden-

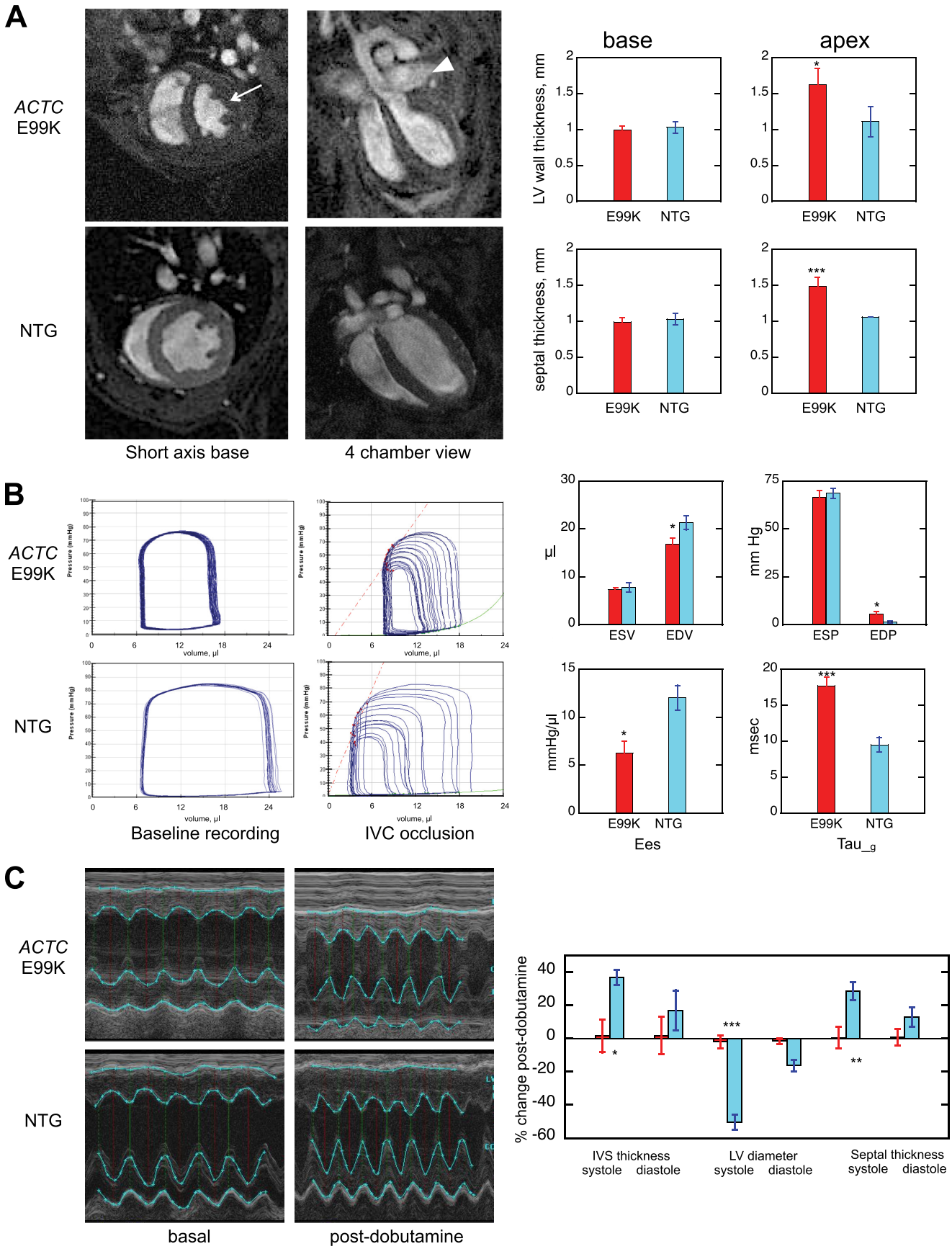
A
ACTC E99K
NTG
Short axis base
4 chamber view
base
apex
LV wall thickness, mm
septal thickness, mm
E99K
NTG
B
ACTC E99K
NTG
Pressure (mmHg)
volume, µl
Baseline recording
IVC occlusion
µl
ESV
EDV
mm Hg
ESP
EDP
mmHg/µl
Ees
msec
Tau_g
C
ACTC E99K
NTG
basal
post-dobutamine
% change post-dobutamine
IVS thickness
systole
diastole
LV diameter
Septal thickness

TABLE 1

The effect of age and gender on cardiac morphology and contraction parameters

Ratio of mean value *ACTC* E99K/NTG is shown, and the statistical significance of the difference is indicated (*, $p = <0.05$; **, $p = <0.01$; and ***, $p = <0.001$). Parameters were measured by MRI (boldface type), echocardiography (italic type), and conductance catheter. Not all parameters were measured for every age and gender. The following abbreviations are used: ED, end-diastolic; ESV, end-systolic volume; EDP, end-diastolic pressure; ESP, end-systolic pressure; P, phosphorylated; dP, dephosphorylated.

Cardiac parameter	Male			Female	
	21 weeks	29 weeks	38 weeks	29 weeks	38 weeks
	%	%	%	%	%
Apical septum thickness ED	**+41*****	**+35****	*+43**	*+81**	
Apical wall thickness ED (LVPW)	**+46***	**+48*****	*+30**	*+40**	
EDV	**−20**** *−21**	**−30*****	+8	+11	+49**
ESV	**+3** *+1*	**−13**	+62*	+53***	+159***
SV	**−34**** *−33**	**−38*****	−20	−44*	−22
EF	**−19****	**−13****	−26*	−36**	−48**
CO	**−47*****	**−42*****	−40**	−50*	−12
EDP	+317**		+82**	+9	+48*
ESP	−2		−6	−5	−1.55
dV/dt_{min}	−34		−35*	−34	−24
dV/dt_{max}	−26		−37*	−26	−21
dP/dt_{min}	−35*		−35	−106***	−32*
dP/dt_{max}	+5		−5	−24	−7
Tau_g	+86***		+132*	+191*	+99*

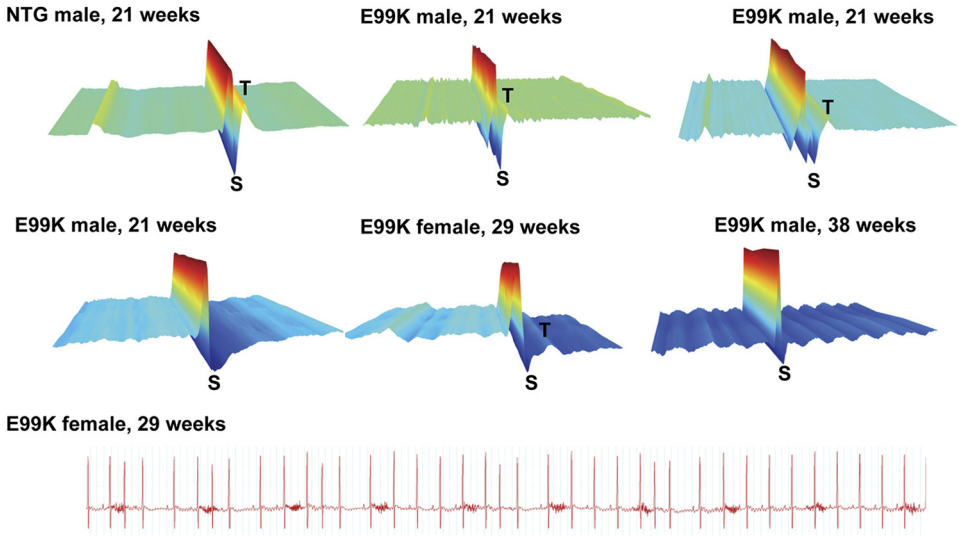

FIGURE 6. **Waterfall plots of ECG recordings.** At least 250 heart cycles are stacked in the *z* axis. *1st row*, from *left to right*: ECG from normal 21-week-old male mice; deep S-wave recorded on 21-week-old male TG mice (double the average normal S amplitude); double S-waves recorded on 21-week-old male mice; *2nd row*, from *left to right*: negative T-wave recorded on 21-week-old male TG mice; negative T-wave recorded on 29-week-old female TG mice; atrial flutter recorded on 38-week-old male TG mice; *3rd row*, atrial ectopic beats recorded on 29-week-old female TG mice.

tifiable in most *ACTC* E99K mice, but QTc was not different from controls (Fig. 6 and supplemental data H).

Echocardiography of β-agonist-stimulated 29-week-old female and 38-week-old male mice revealed a blunted response to β-adrenergic stimulation, with less pronounced increases in heart rate, wall thickening, and fractional shortening compared with NTG mice. Upon β-agonist infusion, QTc increased in NTG mice but was unaltered in *ACTC* E99K mice.

Effects of the ACTC E99K Mutation in the Patient Population—In addition to our measurements on transgenic mice, we also studied heart muscle samples from two patients with the *ACTC* E99K mutation. Patient 1 had a heart transplant, and patient 2 had repairs for an atrial septal defect (supplemental data A). The level of expression, based on two-dimensional electrophoresis (Fig. 1) was 39% in sample 1 and 18% in sample 2. Sample 1 was similar but showed signs of protein degradation and was

FIGURE 5. *A,* MRI imaging. The pictures show short axis sections at the base of the heart and 4-chamber views in diastole. *Arrow* shows thickened wall, and *arrowhead* shows enlarged left atrium. *Graphs* show wall thickness at the base and apex of the hearts (see supplemental data B and C). *B,* pressure-volume loops from 21-week-old male mice at base line and with inferior vena cava transient occlusion. *Graphs* compare calculated end-systolic (*ESV*) and diastolic (*EDV*) volumes, end-systolic (*ESP*) and diastolic (*EDP*) pressures, end-systolic elastance (*Ees*), and Tau_g for ACTC E99K mice and NTG littermates. Details are given in supplemental data D. *C,* M-mode echocardiography traces from 21-week-old male ACTC E99K mice and NTG littermates at base line and after dobutamine infusion. The *graph* shows the calculated percentage change in contractile parameters because of dobutamine for ACTC E99K mice (*red*) and NTG littermates (*light blue*) (see supplemental data E). *LV*, left ventricular; *IVS*, interventricular septum.

TABLE 2

Comparison of molecular phenotype of the *ACTC* E99K mutation in mouse and man

Statistical significance of the difference in ratio relative to 1 is indicated (*, $p = <0.05$; ***, $p = <0.001$). P, phosphorylated; dP, dephosphorylated.

	Expression of mutation (two-dimensional electrophoresis)	Troponin I phosphorylation, 2P-1P-0 ratios and mol of phosphate/mol	Sliding speed, E99K actin/control actin	Ca^{2+} sensitivity, native troponin, EC_{50} E99K actin/ EC_{50} control actin	Ca^{2+} sensitivity, E99K actin, EC_{50} P troponin/EC_{50} dP troponin
Mouse	49.5 ± 4.5%	38:42:21 1.17 mol of phosphate/mol	0.92 ± 0.02*** $p = 0.004$, $n = 14$	0.39 ± 0.09* $p = 0.03$, $n = 5$	1.14 ± 0.06 $p = 0.16$, $n = 4$
Human	39% sample 1 18% sample 2	57:30:13 1.44 mol of phosphate/mol	0.94 ± 0.03*** $p = 0.002$, $n = 10$	0.76 ± 0.05* $p = 0.05$ $n = 4$	0.92 ± 0.21 $n = 3$

not studied further. Measurements of myofibrillar protein phosphorylation in sample 2 were not significantly different from donor heart tissue (Fig. 5) and were also similar to transgenic mice (Table 2).

Functional analysis of pure actin by *in vitro* motility assay showed a 6% reduced sliding speed ($p = 0.002$) in the *ACTC* E99K human heart sample 2 compared with donor heart actin, similar to that observed with the *ACTC* E99K transgenic mice (Table 2 and supplemental data J). To measure Ca^{2+} regulation, actin isolated from sample 2 or donor control muscle was reconstituted with donor heart tropomyosin and troponin. The maximum sliding speed of thin filaments with E99K actin was the same as thin filaments with donor heart actin at both 3.5 and 0.001 μM Ca^{2+}. Ca^{2+} sensitivity of thin filaments containing E99K actin was 32% greater than thin filaments with donor actin, which is a smaller increase than observed with the mouse actin samples (50% mutant) using the same troponin and tropomyosin. We also observed that Ca^{2+} sensitivity of *ACTC* E99K-containing thin filaments was the same with native phosphorylated and dephosphorylated troponin, as was also found with the mouse *ACTC* E99K actin (Fig. 6 and Table 2). The Ca^{2+} sensitivity of E99K-containing thin filaments was 19% greater than donor heart when the troponin was fully dephosphorylated, compared with 18% greater for the mouse E99K thin filaments compared with NTG. Thus, the E99K mutation in human sample 2 increased Ca^{2+} sensitivity and uncoupled Ca^{2+} sensitivity from troponin I phosphorylation in the same way as E99K actin from transgenic mice.

DISCUSSION

ACTC E99K Mouse Model of HCM—We developed the *ACTC E99K* mouse as a model of hypertrophic cardiomyopathy designed to recapitulate the disease found in patients. Cardiac actin is the only contractile protein that has an identical amino acid sequence in humans and mice as well as an identical isoform distribution (80% cardiac actin, *ACTC* and 20% skeletal actin). This is an important property because we have found that the effect of HCM and DCM mutations on function *in vitro* can vary significantly depending on species, isoform, and post-translational modifications (16, 22, 28). Actin transgenes with the MHC promoter lead to substitution of actin rather than overexpression (27), and we observed that myofibrillar protein content is normal (Fig. 3), and there is no unincorporated actin in the cytoplasm. Glutamic acid 99 is located on the surface of the actin monomer on the outside edge of subdomain 1 and is believed to be involved in the initial nonstereo-specific binding of myosin·ADP·P_i to actin during the cross-bridge cycle, consequently the charge-reversal glutamic acid to lysine mutation at this location is expected to produce a phenotype.

Although mutations in *ACTC* are not a common cause of HCM, the clinical consequences of the *ACTC E99K* mutation have been studied in a large population (13). Hypertrophy was reported from 62 of 76 mutation carriers. The distribution of the hypertrophy was predominantly apical. ECG investigation showed abnormalities in 53 of 61 carriers. Atrial fibrillation or flutter was found in 7/53. The 22 adverse events reported included eight sudden deaths (five of which were in a single family). We have been able to study two patient biopsies and make a direct comparison of the molecular phenotype in the patients and the mouse model.

At the single filament level and in skinned papillary muscle, 50% E99K/wild-type actin caused an increase in Ca^{2+} sensitivity of contractile activation. The *ACTC* E99K mice exhibited a remarkable tendency to sudden death at 4–6 weeks old. At 21 weeks, the mice showed hypertrophy, diastolic dysfunction, and fibrosis; at 29–38 weeks, the mice additionally showed evidence of arrhythmia, dilation, and progression to heart failure. Thus, this model reproduces many of the features of hypertrophic cardiomyopathy as found in patients.

Molecular Phenotype of HCM Caused by ACTC E99K Mutation—A higher Ca^{2+} sensitivity of regulation of the contractile apparatus is usually associated with the HCM phenotype (21, 36, 38). This is due to an increased affinity of thin filaments for Ca^{2+} (23, 39), associated with a faster rate of Ca^{2+}-binding to troponin C (40). Higher Ca^{2+} sensitivity was observed in the *ACTC* E99K mouse and in the patient biopsy samples. The 2.3-fold higher Ca^{2+} sensitivity in mouse E99K actin-containing thin filaments may be compared with values of 2.0–2.1-fold with troponin T mutations, measured by IVMA and around 1.5-fold for troponin I mutations measured by ATPase assay (21, 22, 38, 41). The 1.3-fold higher Ca^{2+} sensitivity of isometric force in *ACTC* E99K papillary muscle compares with a mean 1.23-fold higher Ca^{2+} sensitivity observed with a series of seven different HCM mutations in TnI and TnT (21, 36, 42, 43). The increase in Ca^{2+} sensitivity was less with the human heart E99K actin (1.3-fold), which may reflect the lower mutant actin content compared with the mouse E99K actin (Fig. 1).

The higher Ca^{2+} sensitivity in IVMA was a direct result of the mutation because it was observed by comparing thin filaments reconstituted with mutant actin or wild type with the same human heart troponin and tropomyosin. Because the level of MyBP-C and troponin I phosphorylation, which

could also change Ca^{2+} sensitivity, was the same in *ACTC* E99K and NTG mouse muscle, the increased Ca^{2+} sensitivity in skinned papillary muscle must also be a primary effect of the mutation.

A recent IVMA study using baculovirus-expressed E99K actin in combination with bovine cardiac tropomyosin and troponin did not find any shift in Ca^{2+} sensitivity but did observe a reduced sliding speed; however, these discrepancies may be due to using non-human proteins for all three components of the thin filaments (44). This study also revealed reduced thin filament cooperativity; this may influence Ca^{2+} sensitivity under some conditions, although our previous analysis of tropomyosin DCM mutations found no connection between cooperativity and phenotype (23). Studies on the kinetics of baculovirus-expressed E99K actin-activated myosin S-1-ATPase show that the K_m is 4-fold greater than wild type, indicating a weakening of the weak binding interaction between actin and myosin·ADP·P_i (45). This was interpreted as leading to lower force production, but we found the maximum developed pressure in *ACTC* E99K hearts was not different from nontransgenic mice.

In addition, we have demonstrated that the Ca^{2+} sensitivity of E99K actin-containing thin filaments was uncoupled from the PKA-dependent phosphorylation of troponin I. Uncoupling has been reported with other HCM- or DCM-causing mutations in thin filament proteins (16, 28, 46), and in DCM it seems to be the only consistent effect of disease-causing mutations (21). In contrast, HCM mutations are always associated with higher myofibrillar Ca^{2+} sensitivity.

We therefore believe that a constitutively high myofibrillar Ca^{2+} sensitivity is the trigger for the major symptoms of HCM, potentially fatal arrhythmias and hypertrophy of heart muscle. Higher Ca^{2+} sensitivity will impact upon contractility at several points. Most directly, in the absence of compensatory changes in the Ca^{2+} transient, HCM muscle will be hypercontractile with greater force in systole but also impaired relaxation, which could account for diastolic dysfunction. Increased Ca^{2+} sensitivity will also affect the modulation of Ca^{2+} sensitivity by PKA phosphorylation of troponin I (29, 47, 48) (important in the lusitropic response to β-adrenergic stimulation), the length-dependent modulation of Ca^{2+} sensitivity (responsible for the Frank-Starling effect) (49) and intracellular Ca^{2+} homeostasis (50).

Causes of Sudden Death—The *ACTC* E99K transgenic mice show a distinctive progression of the disease phenotype. Particularly striking is the high mortality over short period between 4 and 6 weeks old, which is more pronounced in females (Fig. 1). Because only a proportion of mice die over this short time period and the survivors have almost normal mortality, it is probable that mortality is in part determined by the hybrid genetic background of the C57BL/6xCBA/Ca mice used in this study. There is an interesting parallel in the *ACTC* E99K patient population where 5 of the 8 sudden cardiac deaths recorded were in a single family, again suggesting a strong contribution of genetic background to the propensity for sudden cardiac death. It is notable that the surviving *ACTC* E99K mice showed ECG abnormalities, including spontaneous arrhythmias, suggesting that the mutation *per se* may induce arrhythmias although the sudden death may depend upon additional factors (Fig. 6).

It is likely that the increased probability of arrhythmia, observed in ECG records, is linked to higher myofibrillar Ca^{2+} sensitivity with its associated increased Ca^{2+} buffering in the sarcoplasm. These differences can disturb intracellular Ca^{2+} homeostasis and dynamics leading to alteration of the Ca^{2+} transient, which could influence the shape and duration of the action potential. In troponin T mutant transgenic mice with increased myofibrillar Ca^{2+} sensitivity, the shape of the ventricular action potentials was changed compared with nontransgenic controls, resulting in shorter effective refractory periods, greater beat-to-beat variability of APD, and increased dispersion of ventricular conduction velocities at high heart rates. It was proposed that these changes created an arrhythmogenic substrate (50, 51). This is compatible with our finding that early mortality in *ACTC* E99K mice is twice as frequent in females than males because it is known that female mice have an inherently longer APD that could make the mutation-related alterations in APD worse; moreover, the age of early death corresponds to puberty where the APD lengths of males and females diverge in humans (52, 53).

Hypertrophy in the ACTC E99K Heart—The mechanisms of development of hypertrophy are poorly understood. It is assumed that the same compensatory pathways are involved in physiological exercise hypertrophy and HCM, but in HCM the initiating signal, high myofibrillar Ca^{2+} sensitivity, persists, leading to inappropriate and irreversible hypertrophy.

One hypothesis of the causative pathway was proposed by Watkins and co-workers (54). The hypercontractile phenotype in HCM with impaired relaxation and deranged length-dependent activation leads to inefficient contraction at rest, requiring the consumption of more ATP than usual and compromising the capacity of the cardiomyocyte to maintain energy levels. It was proposed that this could trigger signaling pathways to induce hypertrophy (54).

The *ACTC* E99K mutation is unique among HCM mutations because most patients (57/61) show apical hypertrophy and noncompaction rather than the "classical" septal hypertrophy. This does not seem to be due to genetic background because apical hypertrophy co-segregates with the *ACTC* E99K mutation in families that have unrelated haplotypes (12). In our transgenic mice, hypertrophy was also confined to the apex of the heart, thus confirming that apical hypertrophy is a direct consequence of the *ACTC* E99K mutation. The origin of this specific hypertrophic morphology is currently not known.

The *ACTC* E99K mutation is associated with left ventricular noncompaction as well as hypertrophy, and a minority of cases (10%, including patient 2) also have atrial septal defects, suggesting this mutation may also cause developmental defects (13). We did not see evidence of left ventricular noncompaction in MRI images of our *ACTC* E99K mice, but this abnormal anatomy may not develop, or be undetectable, in the small heart of a mouse. Nearly twice as many nontransgenic as *ACTC* E99K mice were born, which may be indicative of a developmental defect caused by the E99K mutation.

It is interesting to note that HCM in human heart has mostly been studied in tissue obtained from patients with septal thick-

ening who undergo surgery to relieve left ventricular outflow tract obstruction. These septal samples are characterized by a low level of phosphorylation of MyBP-C and troponin I (29, 30, 55–57). In contrast, the two samples examined here, from free wall and from the atrial-septal junction region, showed high levels of phosphorylation similar to those in donor hearts (Fig. 3), and the *ACTC* E99K mouse hearts also had the same high level of phosphorylation as NTG mice. Therefore, the derangement of phosphorylation observed in HCM is a secondary change, perhaps a consequence of the pressure overload that occurs in left ventricular outflow tract obstruction.

There is controversy as to whether donor hearts, with a high level of phosphorylation, are suitable controls because they may not be normal (58). Sample 2 is relevant to this question because this patient had no medication and showed no cardiac dysfunction and could be regarded as having close to a normal heart (supplemental data A). Levels of phosphorylation in this sample were indistinguishable from donor hearts.

Uncoupling of Myofibrillar Ca^{2+} Sensitivity from Troponin I Phosphorylation Level—Our measurements of Ca^{2+} sensitivity, together with measurement and manipulation of troponin I phosphorylation, have revealed that in *ACTC* E99K mice, Ca^{2+} sensitivity is independent of the level of troponin I phosphorylation. Uncoupling was previously reported in the *TNNTI3* R145G mutation (46) and the *TNNC1* L29Q mutation (40) that cause HCM but also in DCM mutations (*ACTC* E361G, *TNNC1* G149D, and *TPM1* E40K (16, 21, 28)) and in troponin from human myectomy samples (56). Thus, it appears that uncoupling may be a default consequence of structural perturbations. A structural model of the interaction between the N terminus of troponin I and troponin C indicates a weak ionic interaction with the Ca^{2+}-binding loop of troponin C, responsible for the high Ca^{2+} sensitivity associated with unphosphorylated troponin I, which is destabilized by phosphorylation (59). We speculate that the *ACTC* E99K mutation causes structural perturbations in the I-C interface that destabilizes this interaction independently of phosphorylation.

Heart Failure in Older Mice—Older *ACTC* E99K mice develop increased end-diastolic and end-systolic volumes, whereas the increased end-diastolic pressure, present in younger mice, is maintained. Interestingly, the dilation develops earlier in females than males (Table 1) and is probably responsible for the higher mortality of older *ACTC* E99K mice compared with nontransgenic littermates. This pattern parallels the development of severe heart failure in a minority of HCM patients (*ACTC* E99K patient 1 is an example), which is related to a combination of severe diastolic dysfunction and moderate systolic dysfunction.

It is noteworthy that uncoupling of Ca^{2+} sensitivity from the troponin I phosphorylation level in the *ACTC* E99K mouse resembles our recent findings with familial DCM mutations. We have proposed that heart failure due to DCM mutations is due to uncoupling causing a blunted response to β-adrenergic stimulation leading to a reduced cardiac reserve (16, 28). The *ACTC* E99K mice clearly show a blunted response to β-adrenergic stimulation (Fig. 5*C*). Thus, uncoupling due to the *ACTC E99K* HCM mutation may contribute to the development of heart failure in older mice.

In conclusion, the *ACTC* E99K transgenic mice reproduce many of the characteristics of hypertrophic cardiomyopathy seen in patients at the single filament and whole animal levels. The variability of the phenotype depending on genetic background, age, and sex and the high rate of sudden death make this a valuable tool for further investigations of the disease process in hypertrophic cardiomyopathy.

Acknowledgments—We acknowledge the help of Valentina Caorsi, Eerke Berger, Ke Liu, Sofia Muses, and Doug Lopes at Imperial College London. Donor heart muscle samples were supplied by Prof. Christobal Dos Remedios, Sydney, Australia.

REFERENCES

1. Force, T., Bonow, R. O., Houser, S. R., Solaro, R. J., Hershberger, R. E., Adhikari, B., Anderson, M. E., Boineau, R., Byrne, B. J., Cappola, T. P., Kalluri, R., LeWinter, M. M., Maron, M. S., Molkentin, J. D., Ommen, S. R., Regnier, M., Tang, W. H., Tian, R., Konstam, M. A., Maron, B. J., and Seidman, C. E. (2010) *Circulation* **122,** 1130–1133
2. Maron, B. J. (2002) *JAMA* **287,** 1308–1320
3. Richard, P., Charron, P., Carrier, L., Ledeuil, C., Cheav, T., Pichereau, C., Benaiche, A., Isnard, R., Dubourg, O., Burban, M., Gueffet, J. P., Millaire, A., Desnos, M., Schwartz, K., Hainque, B., and Komajda, M. (2003) *Circulation* **107,** 2227–2232
4. Van Driest, S. L., Ellsworth, E. G., Ommen, S. R., Tajik, A. J., Gersh, B. J., and Ackerman, M. J. (2003) *Circulation* **108,** 445–451
5. Van Driest, S. L., Jaeger, M. A., Ommen, S. R., Will, M. L., Gersh, B. J., Tajik, A. J., and Ackerman, M. J. (2004) *J. Am. Coll. Cardiol.* **44,** 602–610
6. Van Driest, S. L., Vasile, V. C., Ommen, S. R., Will, M. L., Tajik, A. J., Gersh, B. J., and Ackerman, M. J. (2004) *J. Am. Coll. Cardiol.* **44,** 1903–1910
7. Olivotto, I., Girolami, F., Ackerman, M. J., Nistri, S., Bos, J. M., Zachara, E., Ommen, S. R., Theis, J. L., Vaubel, R. A., Re, F., Armentano, C., Poggesi, C., Torricelli, F., and Cecchi, F. (2008) *Mayo Clin. Proc.* **83,** 630–638
8. Kaski, J., Syrris, P., Tome Esteban, M., Jenkins, S., Pantazis, A., Deanfield, J., McKenna, W., and Elliott, P. (2009) *Circulation: Cardiovascular Genetics* **2,** 436–441
9. Olson, T. M., Doan, T. P., Kishimoto, N. Y., Whitby, F. G., Ackerman, M. J., and Fananapazir, L. (2000) *J. Mol. Cell. Cardiol.* **32,** 1687–1694
10. Mogensen, J., Perrot, A., Andersen, P. S., Havndrup, O., Klausen, I. C., Christiansen, M., Bross, P., Egeblad, H., Bundgaard, H., Osterziel, K. J., Haltern, G., Lapp, H., Reinecke, P., Gregersen, N., and Børglum, A. D. (2004) *J. Med. Genet.* **41,** e10
11. Morita, H., Rehm, H. L., Menesses, A., McDonough, B., Roberts, A. E., Kucherlapati, R., Towbin, J. A., Seidman, J. G., and Seidman, C. E. (2008) *N. Engl. J. Med.* **358,** 1899–1908
12. Arad, M., Penas-Lado, M., Monserrat, L., Maron, B. J., Sherrid, M., Ho, C. Y., Barr, S., Karim, A., Olson, T. M., Kamisago, M., Seidman, J. G., and Seidman, C. E. (2005) *Circulation* **112,** 2805–2811
13. Monserrat, L., Hermida-Prieto, M., Fernandez, X., Rodríguez, I., Dumont, C., Cazón, L., Cuesta, M. G., Gonzalez-Juanatey, C., Peteiro, J., Alvarez, N., Penas-Lado, M., and Castro-Beiras, A. (2007) *Eur. Heart J.* **28,** 1953–1961
14. Elliott, P., and McKenna, W. J. (2004) *Lancet* **363,** 1881–1891
15. Bottinelli, R., Coviello, D. A., Redwood, C. S., Pellegrino, M. A., Maron, B. J., Spirito, P., Watkins, H., and Reggiani, C. (1998) *Circ. Res.* **82,** 106–115
16. Dyer, E. C., Jacques, A. M., Hoskins, A. C., Ward, D. G., Gallon, C. E., Messer, A. E., Kaski, J. P., Burch, M., Kentish, J. C., and Marston, S. B. (2009) *Circ. Heart Fail.* **2,** 456–464
17. Nier, V., Schultz, I., Brenner, B., Forssmann, W., and Raida, M. (1999) *FEBS Lett.* **461,** 246–252
18. Redwood, C. S., Moolman-Smook, J. C., and Watkins, H. (1999) *Cardiovasc. Res.* **44,** 20–36
19. Knollmann, B. C., and Potter, J. D. (2001) *Trends Cardiovasc. Med.* **11,** 206–212
20. Seidman, J. G., and Seidman, C. (2001) *Cell* **104,** 557–567
21. Marston, S. B. (2011) *J. Cardiovasc. Transl. Res.* **4,** 245–255

22. Redwood, C., Lohmann, K., Bing, W., Esposito, G. M., Elliott, K., Abdulrazzak, H., Knott, A., Purcell, I., Marston, S., and Watkins, H. (2000) *Circ. Res.* **86,** 1146–1152
23. Mirza, M., Robinson, P., Kremneva, E., Copeland, O., Nikolaeva, O., Watkins, H., Levitsky, D., Redwood, C., El-Mezgueldi, M., and Marston, S. (2007) *J. Biol. Chem.* **282,** 13487–13497
24. Rubenstein, P. A., and Martin, D. J. (1983) *J. Biol. Chem.* **258,** 11354–11360
25. Suurmeijer, A. J., Clément, S., Francesconi, A., Bocchi, L., Angelini, A., Van Veldhuisen, D. J., Spagnoli, L. G., Gabbiani, G., and Orlandi, A. (2003) *J. Pathol.* **199,** 387–397
26. Copeland, O., Nowak, K. J., Laing, N. G., Ravenscroft, G., Messer, A. E., Bayliss, C. R., and Marston, S. B. (2010) *J. Muscle Res. Cell Motil.* **31,** 207–214
27. Kumar, A., Crawford, K., Flick, R., Klevitsky, R., Lorenz, J. N., Bove, K. E., Robbins, J., and Lessard, J. L. (2004) *Transgenic. Res.* **13,** 531–540
28. Song, W., Dyer, E., Stuckey, D., Leung, M. C., Memo, M., Mansfield, C., Ferenczi, M., Liu, K., Redwood, C., Nowak, K., Harding, S., Clarke, K., Wells, D., and Marston, S. (2010) *J. Mol. Cell. Cardiol.* **49,** 380–389
29. Messer, A. E., Jacques, A. M., and Marston, S. B. (2007) *J. Mol. Cell. Cardiol.* **42,** 247–259
30. Messer, A. E., Gallon, C. E., McKenna, W. J., Dos Remedios, C. G., and Marston, S. B. (2009) *Proteomics Clin. Appl.* **3,** 1371–1382
31. Knott, A., Purcell, I., and Marston, S. (2002) *J. Mol. Cell. Cardiol.* **34,** 469–482
32. Bing, W., Fraser, I. D., and Marston, S. B. (1997) *Biochem. J.* **327,** 335–340
33. Fraser, I. D., and Marston, S. B. (1995) *J. Biol. Chem.* **270,** 7836–7841
34. Marston, S. B., Fraser, I. D., Bing, W., and Roper, G. (1996) *J. Muscle Res. Cell Motil.* **17,** 497–506
35. Marston, S. (2003) *J. Muscle Res. Cell Motil.* **24,** 149–156
36. Takahashi-Yanaga, F., Morimoto, S., Harada, K., Minakami, R., Shiraishi, F., Ohta, M., Lu, Q. W., Sasaguri, T., and Ohtsuki, I. (2001) *J. Mol. Cell. Cardiol.* **33,** 2095–2107
37. Jacoby, C., Molojavyi, A., Flögel, U., Merx, M. W., Ding, Z., and Schrader, J. (2006) *Basic Res. Cardiol.* **101,** 87–95
38. Robinson, P., Mirza, M., Knott, A., Abdulrazzak, H., Willott, R., Marston, S., Watkins, H., and Redwood, C. (2002) *J. Biol. Chem.* **277,** 40710–40716
39. Robinson, P., Griffiths, P. J., Watkins, H., and Redwood, C. S. (2007) *Circ. Res.* **101,** 1266–1273
40. Dong, W. J., Xing, J., Ouyang, Y., An, J., and Cheung, H. C. (2008) *J. Biol. Chem.* **283,** 3424–3432
41. Elliott, K., Watkins, H., and Redwood, C. S. (2000) *J. Biol. Chem.* **275,** 22069–22074
42. Szczesna, D., Zhang, R., Zhao, J., Jones, M., Guzman, G., and Potter, J. D. (2000) *J. Biol. Chem.* **275,** 624–630
43. Lu, Q. W., Morimoto, S., Harada, K., Du, C. K., Takahashi-Yanaga, F., Miwa, Y., Sasaguri, T., and Ohtsuki, I. (2003) *J. Mol. Cell. Cardiol.* **35,** 1421–1427
44. Debold, E. P., Saber, W., Cheema, Y., Bookwalter, C. S., Trybus, K. M., Warshaw, D. M., and Vanburen, P. (2010) *J. Mol. Cell. Cardiol.* **48,** 286–292
45. Bookwalter, C. S., and Trybus, K. M. (2006) *J. Biol. Chem.* **281,** 16777–16784
46. Deng, Y., Schmidtmann, A., Redlich, A., Westerdorf, B., Jaquet, K., and Thieleczek, R. (2001) *Biochemistry* **40,** 14593–14602
47. Layland, J., Solaro, R. J., and Shah, A. M. (2005) *Cardiovasc. Res.* **66,** 12–21
48. van der Velden, J., de Jong, J. W., Owen, V. J., Burton, P. B., and Stienen, G. J. (2000) *Cardiovasc. Res.* **46,** 487–495
49. de Tombe, P., Mateja, R. D., Tachampa, K., Mou, Y. A., Farman, G. P., and Irving, T. C. (2010) *J. Mol. Cell. Cardiol.* **45,** 851–858
50. Huke, S., and Knollmann, B. C. (2010) *J. Mol. Cell. Cardiol.* **48,** 824–833
51. Baudenbacher, F., Schober, T., Pinto, J. R., Sidorov, V. Y., Hilliard, F., Solaro, R. J., Potter, J. D., and Knollmann, B. C. (2008) *J. Clin. Invest.* **118,** 3893–3903
52. James, A. F., Choisy, S. C., and Hancox, J. C. (2007) *Prog. Biophys. Mol. Biol.* **94,** 265–319
53. Mason, S. A., and MacLeod, K. T. (2009) *Biochem. Biophys. Res. Commun.* **388,** 565–570
54. Ashrafian, H., Redwood, C., Blair, E., and Watkins, H. (2003) *Trends Genet.* **19,** 263–268
55. Hoskins, A. C., Jacques, A., Bardswell, S. C., McKenna, W. J., Tsang, V., dos Remedios, C. G., Ehler, E., Adams, K., Jalilzadeh, S., Avkiran, M., Watkins, H., Redwood, C., Marston, S. B., and Kentish, J. C. (2010) *J. Mol. Cell. Cardiol.* **49,** 737–745
56. Jacques, A., Hoskins, A., Kentish, J., and Marston, S. B. (2009) *J. Muscle Res. Cell Motil.* **29,** 239–246
57. Zaremba, R., Merkus, D., Hamdani, N., Lamers, J. M., Paulus, W. J., Dos Remedios, C., Duncker, D. J., Stienen, G. J., and van der Velden, J. (2007) *Proteomics Clin. Appl.* **1,** 1285–1290
58. Jweied, E., deTombe, P., and Buttrick, P. M. (2007) *J. Mol. Cell. Cardiol.* **42,** 722–726
59. Howarth, J. W., Meller, J., Solaro, R. J., Trewhella, J., and Rosevear, P. R. (2007) *J. Mol. Biol.* **373,** 706–722
60. Pirani, A., Vinogradova, M. V., Curmi, P. M., King, W. A., Fletterick, R. J., Craig, R., Tobacman, L. S., Xu, C., Hatch, V., and Lehman, W. (2006) *J. Mol. Biol.* **357,** 707–717